

# Sequence-specific DNA strand cleavage by $^{111}\text{In}$ -labeled peptide nucleic acids

Yujian He<sup>1</sup>, Igor G. Panyutin<sup>1</sup>, Alex Karavanov<sup>2</sup>, Vadim V. Demidov<sup>3</sup>, Ronald D. Neumann<sup>1</sup>

<sup>1</sup> Department of Nuclear Medicine, Warren G. Magnuson Clinical Center, National Institutes of Health, Bethesda, USA

<sup>2</sup> CIPHERGEN BioSystems Inc., Fremont, CA, USA

<sup>3</sup> Center for Advanced Biotechnology, Boston University, Boston, USA

Received: 15 September 2003 / Accepted: 9 December 2003 / Published online: 5 February 2004

© Springer-Verlag 2004

**Abstract.** Peptide nucleic acids (PNAs) bind tightly and sequence-specifically to single- and double-stranded nucleic acids, and are hence of interest in the design of gene-targeted radiotherapeutics that could deliver the radiodamage to designated DNA and/or RNA sites. As a first step towards this goal, we developed a procedure for incorporation of Auger electron-emitting radionuclide (indium-111) into PNA oligomers and studied the efficiency of PNA-directed cleavage of single-stranded DNA targets. Accordingly, diethylene triamine pentaacetic acid (DTPA) was conjugated to the lysine-appended mixed-base PNAs and sequence-homologous DNA oligomer with a proper linker for comparative studies. By chelation of PNA-DTPA and DNA-DTPA conjugates with  $^{111}\text{In}^{3+}$  in acidic aqueous solutions,  $^{111}\text{In}$ -labeled PNA and DNA oligomers were obtained. Targeting of single-stranded DNA with PNA-DTPA- $^{111}\text{In}$  conjugates yielded highly localized DNA strand cleavage; the distribution of breaks along the target DNA strand has two maxima corresponding to both termini of PNA oligomer. After 10–14 days, the overall yield of breaks thus generated within the PNA-targeted DNA by  $^{111}\text{In}$  decay was 5–7% versus  $\leq 2\%$  in the case of control oligonucleotide DNA-DTPA- $^{111}\text{In}$ . The estimated yield of DNA strand breaks per nuclear decay is  $\sim 0.1$  for the PNA-directed delivery of  $^{111}\text{In}$ , which is three times more than for the DNA-directed delivery of this radionuclide. This *in vitro* study shows that  $^{111}\text{In}$ -labeled PNAs are much more effective than radiolabeled DNA oligonucleotides for site-specific damaging of DNA targets. Accordingly, we believe that PNA oligomers are promising radionuclide delivery tools for future antisense/antigene radiotherapy trials.

**Keywords:** DTPA –  $^{111}\text{In}$  – Peptide nucleic acids – DNA damage – Gene targeting

**Eur J Nucl Med Mol Imaging (2004) 31:837–845**

DOI 10.1007/s00259-003-1446-0

## Introduction

Radiotherapy represents one of the most common methods for clinical treatment of malignant tumors and it has been refined intensely and improved in the past decade. Rational delivery of therapeutic radiation only to the target cancer cells is an important research strategy for the field of radiation oncology [1, 2, 3]. To this end, design of gene-targeted radiopharmaceuticals is warranted as a possible approach for radionuclide and radiotherapy on a molecular level [4, 5]. Correspondingly, we are investigating a technique for molecular level radiotherapy called antisense/antigene radiotherapy, which is based on the site-specific targeting of genetic sequences in the form of single- and double-stranded nucleic acids with radiolabeled oligonucleotides [6, 7, 8, 9, 10, 11, 12, 13, 14, 15, 16, 17, 18].

In the antisense/antigene radiotherapy approach, duplex- and triplex-forming oligodeoxyribonucleotides (ODNs) are designed as carrier molecules to selectively deliver short-range, Auger electron-emitting radionuclides, such as iodine-125, iodine-123, or indium-111, to a designated DNA/RNA sequence from cellular oncogenes via site-specific duplex or triplex formation [9, 14, 16, 17]. In this way, more of the lethal radiodamaging effects of the Auger electron emitters are precisely directed within the affected cells to particular mRNA or genomic DNA sites, while producing minimal damage to the rest of the genome and to other cellular components [14, 16].

Notwithstanding the successful proof-of-principle demonstration of this technique in several model studies

Igor G. Panyutin (✉)

Department of Nuclear Medicine,  
Warren G. Magnuson Clinical Center,  
National Institutes of Health, Bethesda,  
MD 20892-1180, USA

e-mail: igorp@helix.nih.gov

Tel.: +1-301-4968308, Fax: +1-301-4809712

[6, 7, 8, 10, 11, 12, 13, 15, 17, 18], the antisense/antigene radiotherapy approach needs further advances to be positively considered for clinical trials. One of the possible improvements is to replace the ordinary oligonucleotides, used as molecular vehicles for target-mediated radionuclide delivery, by nonionic peptide nucleic acid (PNA) oligomers [19, 20, 21, 22, 23]. Indeed, such a replacement may provide the antisense/antigene radiotherapy approach with better sequence specificity intrinsic to PNA [20, 24, 25] along with an enhanced stability of hybrid duplexes and triplexes formed by PNA oligomers with DNA and RNA targets [20, 21, 23, 26]. Because PNA has the non-natural polyamide (pseudopeptide) backbone instead of the sugar-phosphate backbone of natural nucleic acids, PNAs exhibit much higher chemical and biological stability [21, 27, 28, 29] compared with the biodegradable nuclease-sensitive natural oligonucleotides [10, 21, 28]. In addition, PNA oligomers can selectively target double-stranded DNA via duplex- or triplex-invasion modes [21, 23, 26].

In view of this potential of PNA for use in antisense/antigene radiotherapy, we developed a procedure for labeling of PNA oligomers with radionuclides. Short half-life (2.8 days)  $^{111}\text{In}$  was used in this study as a clinically convenient Auger electron emitter [11, 12]. We also analyze in this paper the yield and sequence specificity of breaks produced within single-stranded DNA after its *in vitro* targeting with radiolabeled PNAs. Our study demonstrates that  $^{111}\text{In}$ -labeled PNAs are three times more effective for site-specific damaging of DNA targets than similarly labeled natural oligonucleotides.

## Materials and methods

**DNA and PNA oligomers.** The ODNs (Table 1) were synthesized on an ABI394 DNA synthesizer (Applied Biosystems, Foster City, CA). They were further purified by high-performance liquid chromatography (HPLC) and polyacrylamide gel electrophoresis (PAGE) before conjugation, as described elsewhere [6, 12]. The PAGE experiments used standard protocols, and the TBE buffer (89 mM Tris base–89 mM boric acid–2 mM disodium EDTA, pH 8) was used as the running buffer. The HPLC (Model 1050, Hewlett Packard, Palo Alto, CA) was performed at a flow rate of 0.7 ml/min with a linear gradient of 0.1 M triethylamine acetate (TEAA, pH 7.5) and acetonitrile (ACN) from 95/5 to 15/85 (v/v) for 45 min at room temperature, using a reverse phase PRP-1

Hamilton C18 column (150×4.6 mm). The ODN concentrations were calculated spectrophotometrically with biopolymer calculator software (<http://paris.chem.yale.edu/extinct.html>).

The sequence-homologous 15-mer PNA 1 (H-TAGTTATCTCT-ATCT-Lys-NH<sub>2</sub>) and PNA 2 (H-TAGTTATCTCTATCT-Lys<sub>3</sub>-NH<sub>2</sub>) were purchased from Applied Biosystems. The PNA oligomer that we used features a mixed-base “random” sequence with low purine content to avoid any possible solubility/aggregation problems. According to nomenclature accepted for PNA structure, H- and -NH<sub>2</sub> denote the N-terminal amino group and C-terminal amido group, respectively. A small amount of PNA 1 was gifted by Dr. P.E. Nielsen (Copenhagen University, Denmark) for our pilot experiments. The PNA samples were further purified with HPLC at a flow rate of 0.7 ml/min with a linear gradient of solvent A [0.1% trifluoroacetic acid (TFA) in 100% ACN] and solvent B (0.1% TFA in 1% ACN) from 1/99 to 100/0 (v/v) for 45 min at 55°C, also using a reverse phase PRP-1 Hamilton C18 column (150×4.6 mm). The PNA concentrations were calculated spectrophotometrically using the sum of extinction coefficients (A=13.7, G=11.7, T=8.6, and C=6.6 ml/μmol×cm at 260 nm) for the given PNA sequence [30, 31].

**Conjugation of diethylene triamine penta-acetic acid (DTPA) with PNA.** Two microliters of 1.25 M NaHCO<sub>3</sub> buffer (pH 8.5) and 2 μl of a fresh solution of cyclic DTPA dianhydride (cDTPAA) (Sigma, St. Louis, MO) in anhydrous DMSO (~400 nmol cDTPAA) were added to 1 nmol dried PNA in a 0.5 ml low-adhesion polypropylene micro centrifuge tube. The mixture was shaken at room temperature (~22°C) overnight. After reaction, the DTPA-conjugated PNA (or DNA) was purified by HPLC so that the free DTPA was removed completely. The HPLC conditions were as above for DNA HPLC purification. The peak at approximately 10 min retention time was collected, and the sample was evaporated to dryness. A stock solution of PNA-DTPA conjugates was prepared in 0.2 M sodium acetate and 0.02 M sodium citrate buffer (pH 4.5) that was pretreated with Chelex 100 resin to remove multivalent metal cations [12].

Gel shift analysis of PNA with DTPA conjugation was performed in 12% nondenaturing PAGE at 4°C. The target DNA2 was labeled with fluorescein, and the bands could be directly visualized and quantitated using a fluorimager (model 595, Molecular Dynamics, Sunnyvale, CA).

The surface-enhanced laser desorption/ionization mass spectrometry (SELDI-MS) analysis of PNA with DTPA conjugation was measured on a Ciphergen proteinChip System (Ciphergen Biosystems, Inc., Fremont, CA). H4 chips were used for both DNA and PNA samples. A 1-μl sample (10 μM) was dropped to a chip spot prewashed with ACN. After the sample had been air-dried, 0.3 μl 3-hydroxypicolinic acid solution (HPA), as matrix, was added to the spot. After 10 min, an additional 0.3 μl of HPA was added and dried, and the mass spectra were determined. The

**Table 1.** Composition of PNAs and control/target DNAs<sup>a, b</sup>

PNA 1:	H-TAGTTATCTCTATCT-Lys-NH <sub>2</sub>
PNA 2:	H-TAGTTATCTCTATCT-Lys-Lys-Lys-NH <sub>2</sub>
Control DNA:	H <sub>2</sub> N-C <sub>6</sub> H <sub>12</sub> -TAGTTATCTCTATCT
Target DNA 1:	TTGAGATTACACAGATAGAGATAACTAGATACTTACGAC
Target DNA 2:	TTGAGATTACACAGATAGAGATAA-CTAGATACTTACGAC-fluorescein

Lys, Lysine

<sup>a</sup> PNA sequences are written from N- to C-terminus

<sup>b</sup> DNA sequences are written from the 5'- to the 3'-end and the PNA binding site is shown in bold letters

HPA solution was made by 15 mg HPA mixed with 100  $\mu$ l ACN, 80  $\mu$ l H<sub>2</sub>O, and 20  $\mu$ l 0.5 M ammonium citrate.

Ion-exchange HPLC was also used to monitor the conjugation of DTPA with PNA. It was performed using an anion-exchange column (7.5 mm $\times$ 4.6 mm, Nucleogen-Deae 60-7, Macherey-Nagel, Germany) at a flow rate of 0.7 ml/min with a linear gradient of 0.02 M KH<sub>2</sub>PO<sub>4</sub> in 20% ACN (pH 7.0) and 0.02 M KH<sub>2</sub>PO<sub>4</sub>-1 M KCl in 20% ACN (pH 7.0) (aqueous) from 90/10 to 48/52 over 60 min at 55°C, and detected at 260 nm. The percent of PNA conjugated to DTPA was obtained by measuring the areas under corresponding peaks in the chromatogram.

**Preparation of <sup>111</sup>In-labeled PNA.** Nine and one-half pmol (~14.8 MBq in 1  $\mu$ l) of fresh <sup>111</sup>In<sup>3+</sup> in 0.05 N HCl (PerkinElmer, Boston, MA) was added to 5 pmol (1.2  $\mu$ l, 4.4  $\mu$ M) PNA-DTPA or 5 pmol control DNA-DTPA (0.77  $\mu$ l 6.5  $\mu$ M) in 0.2 M sodium acetate and 0.02 M sodium citrate buffer (pH 4.5) that was demetalized by Chelex 100 resin. The samples were incubated for 10 min at room temperature; further incubation did not result in a significant increase in <sup>111</sup>In incorporation. Then, the reactions were quenched with 1  $\mu$ l 0.2 mM DTPA. The extent of <sup>111</sup>In<sup>3+</sup> binding to PNA-DTPA or DNA-DTPA was determined by denaturing 12% PAGE.

**ODN labeling by <sup>32</sup>P and complexing with <sup>111</sup>In-labeled PNA.** Oligomeric target DNA was labeled at the 5' end with [<sup>32</sup>P]- $\gamma$ -ATP using T4 polynucleotide kinase, or at the 3' end with [<sup>32</sup>P]- $\alpha$ -ATP using terminal deoxynucleotidyl transferase (TdT), and purified on MicroSpin G50 columns (Amersham Pharmacia Biotech Inc, Piscataway, NJ) according to the manufacturer's protocol. Their final concentrations (~0.2 pmol/ $\mu$ l) were determined spectrophotometrically as described above.

<sup>111</sup>In-labeled PNA was mixed with the complementary oligomeric target DNA in STE buffer (50 mM Tris/HCl-50 mM NaCl-1 mM EDTA, pH 7.4) at a ratio of 2:1 (mol/mol). The mixture was incubated at room temperature for 10 min, then was analyzed in a 20% nondenaturing PAGE at 4°C to check whether the duplex had formed. Duplex samples were frozen at -80°C for DNA damage accumulation. Alternatively, the target DNA was labeled with fluorescein at the 3' end. The PNA/DNA duplex formation and DNA strand break analyses were done using nondenaturing and denaturing PAGE, respectively.

**DNA strand break analysis.** After 10-14 days, the duplex samples were thawed and purified using G-25 spin columns twice to remove free <sup>111</sup>In and other small molecules, and the strand break yield was determined in a 20% denaturing PAGE. The DNA strand breaks were quantified using a FUJIFILM BAS-1500 Bioimager (FUJIFILM Medical Systems USA, Stamford, CT). To measure the intensity of the individual bands, the intensity profile of each lane was generated from the digitized gel image using Fuji Lab Image Gauge software (FUJI Medical Systems USA). The profile was deconvoluted to a series of the Lorentz-type peaks corresponding to individual bands as described in detail in reference [15]. The best-fit curves were produced with PeakFit software package for PC (SPSS Inc., Richmond, CA).

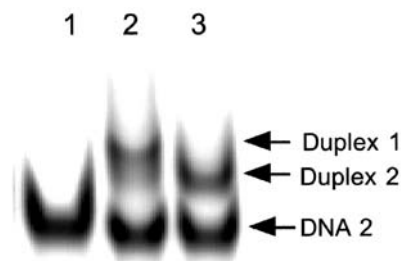


**Fig. 1.** Assay for PNA-DTPA conjugation by 12% nondenaturing PAGE at 4°C. Lanes: 1, target DNA 2; 2, PNA 1-DTPA + target DNA 2; 3, PNA 1 + target DNA 2. Binding of PNA 1-DTPA conjugate to DNA2 results in larger retardation in the gel (band Duplex 1, lane 2) as compared to binding of PNA 1 alone (band Duplex 2, lane 3)

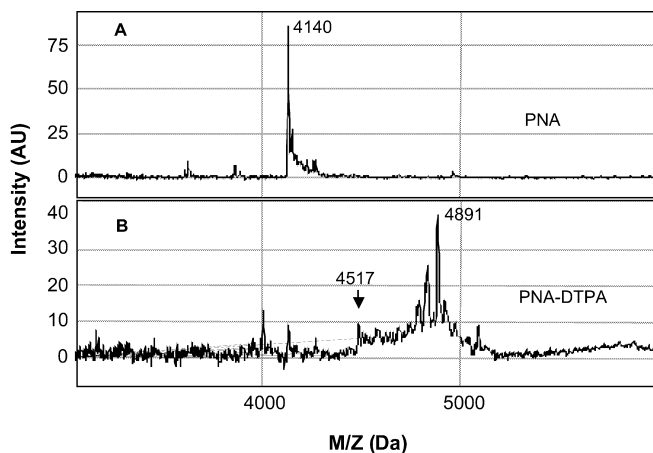
## Results and discussion

### Conjugation of DTPA to PNA

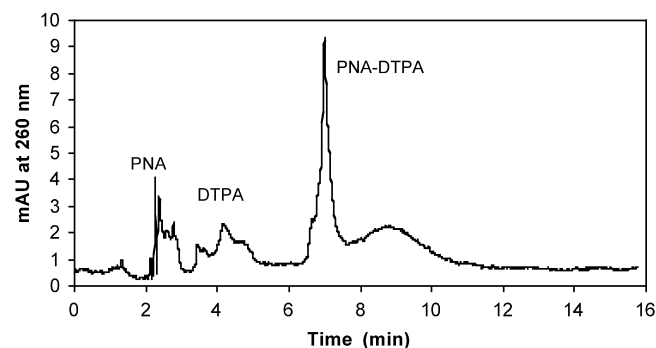
DTPA was initially conjugated to amino groups of PNA 1 (Table 1) at the carboxy (the side-chain lysine amino group) and/or amino (the end-located backbone amino group) termini via the acylation reaction [32, 33]. Three different methods were applied to monitor the conjugation reaction. The conjugation yield was first determined by gel electrophoresis. Since PNA 1 is poorly charged (it consists of a neutral backbone and carries two positive terminal charges), it migrates very slowly during electrophoresis. Therefore, to detect a change in electrophoretic mobility caused by PNA conjugation with DTPA, we annealed the PNA to a complementary DNA strand labeled with fluorescein to increase the PNA gel mobility.

Figure 1 shows the results of such a band-shift experiment. Binding of PNA to target DNA 2 resulted in the appearance of slow-migrating bands in lanes 2 and 3. The band corresponding to the duplex formed between target DNA 2 and PNA-DTPA conjugate is shifted up in the gel (Duplex 1, lane 2) relative to the band corresponding to the target DNA 2/PNA duplex (Duplex 2, lane 3). Conjugation yield was measured as a ratio of the intensity of the shifted (Duplex 1) to the total of the shifted and the original (Duplex 2) bands in line 2 and was estimated to be >90%. The conjugation yield of control DNA oligonucleotide was assessed by denaturing PAGE using <sup>32</sup>P labeling, as was reported previously [12], and a conjugation yield close to 100% was determined.

SELDI-MS can directly determine the conjugation of PNA 1 via comparison of the mass change between the PNA and PNA-DTPA (Fig. 2). The mass of the major PNA 1 peak is 4,140 (Fig. 2A); after conjugation this peak disappears, and a group of new peaks appears around a major mass peak at 4,891 (Fig. 2B). Attachment of cDTPAA would result in a mass increase by 357 (cDTPAA M.W.=357). However, one of the two anhy-



**Fig. 2A, B.** Mass spectrometry analysis of PNA 1-DTPA conjugation: **A** PNA 1 before conjugation; **B** PNA 1 after conjugation. AU, Arbitrary units



**Fig. 3.** Ion-exchange HPLC profile of PNA 1-DTPA conjugation. mAU, Milliabsorbance units

dride rings of cDTPAA can be easily opened via hydrolysis to result in an additional mass increase of 18 Da; thus the total increase would be 375. There is a minor peak at 4,517 corresponding to conjugation of PNA 1 with one cDTPAA. Conjugation with two cDTPAAs would result in the product with mass 4,890. The major observed peak at 4,891 is very close to that predicted value. There are also other peaks around the major peak at 4,891 that can be attributed to an incomplete opening of DTPAA rings or to modifications of PNA-DTPA conjugate during ionization that are often observed on the matrix-assisted mass spectra of oligonucleotides [34]. Nevertheless, the SELDI-MS data clearly demonstrated that the majority of PNA molecules were conjugated with two cDTPAA molecules. The fact that two DTPA molecules can be conjugated to one PNA molecule implies that there may be two  $^{111}\text{In}$  binding sites in PNA-DTPA.

Ion-exchange HPLC was also used to assess the percentage of PNA 1 conjugated to DTPA (Fig. 3). In Fig. 3, PNA-DTPA complex has a peak with a larger retention time than free PNA or free DTPA, corresponding

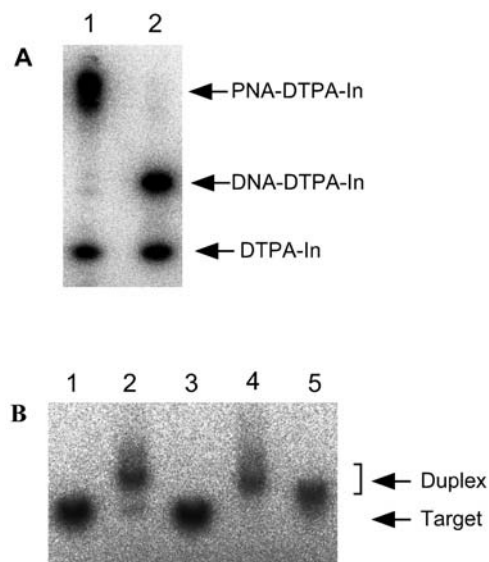


**Fig. 4 A.**  $^{111}\text{In}$  labeling of PNA 1-DTPA and control DNA-DTPA conjugation via 12% denaturing PAGE (4°C). Lanes: 1, PNA 1-DTPA +  $^{111}\text{In}^{3+}$ ; 2, control DNA-DTPA +  $^{111}\text{In}^{3+}$ . **B** Binding of PNA 1-DTPA- $^{111}\text{In}$  to target DNA via 20% native PAGE (4°C). Lanes: 1, target DNA 1- $^{32}\text{P}$ -3'; 2, PNA 1-DTPA- $^{111}\text{In}$  + target DNA 1- $^{32}\text{P}$ -3'; 3, target DNA 1- $^{32}\text{P}$ -5'; 4, PNA 1-DTPA- $^{111}\text{In}$  + target DNA 1- $^{32}\text{P}$ -5'; 5, control DNA-DTPA- $^{111}\text{In}$  + target DNA 1- $^{32}\text{P}$ -5'

to the PNA-DTPA conjugates at ~7.5 min. According to the areas of corresponding peaks in the chromatogram, the conjugation yield was estimated as ~86%. The sum of these data demonstrate that PNA 1 was effectively conjugated with cDTPAA at pH 8–9.

We performed the DTPA conjugation to PNA or DNA at a molar ratio of cDTPAA to PNA or DNA equal to 400. We optimized the concentration of PNA or DNA and the pH of the reaction to minimize the formation of the intermolecular cross-linking of two PNA molecules to one cDTPAA molecule. In this study, the separation of PNA-DTPA from the excess of free DTPA in the conjugation reaction solution was performed by HPLC using the same conditions as above to eliminate the effect of free DTPA in the binding of  $^{111}\text{In}$  to PNA-DTPA. Under the optimized conjugation/separation conditions, the retention time of the free DTPA was ~2.5 min, and that of PNA-DTPA was 8.5 min; thus, they could be easily separated.

#### Binding yields of $^{111}\text{In}$ to PNA-DTPA

Binding of  $^{111}\text{In}$  to PNA-DTPA was monitored by PAGE (Fig. 4A). The PNA-DTPA- $^{111}\text{In}$  displayed an unusually bigger band compared with DNA. This may reflect a smaller charge of the PNA molecule as compared to the DNA molecule. Lane 1 in Fig. 4A shows the ability of  $^{111}\text{In}$  to bind to PNA-DTPA after HPLC purifica-

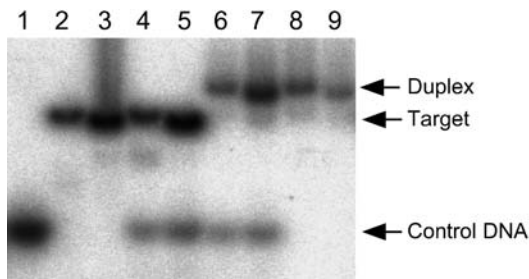


**Fig. 5.** The binding efficiency of PNA and control DNA to target DNA 1 to form duplex via 20% nondenaturing PAGE at room temperature ( $\sim 22^\circ\text{C}$ ). *Lanes:* 1, control DNA- $^{32}\text{P}$ -3'; 2, target DNA 1- $^{32}\text{P}$ -3'; 3, target DNA 1- $^{32}\text{P}$ -5'; 4, control DNA- $^{32}\text{P}$ -3' + target DNA 1- $^{32}\text{P}$ -3'; 5, control DNA- $^{32}\text{P}$ -3' + target DNA 1- $^{32}\text{P}$ -5'; 6, control DNA- $^{32}\text{P}$ -3' + target DNA 1- $^{32}\text{P}$ -3' + cold PNA 1; 7, control DNA- $^{32}\text{P}$ -3' + target DNA 1- $^{32}\text{P}$ -5' + cold PNA 1; 8, target DNA- $^{32}\text{P}$ -3' + cold PNA 1; 9, target DNA- $^{32}\text{P}$ -5' + cold PNA 1

tion. The initial molar ratio of  $^{111}\text{In}$  to PNA-DTPA was 1.9:1; since 42% of  $^{111}\text{In}$  was associated with the PNA-DTPA band, we estimated that approximately 80% of the PNA-DTPA conjugates were labeled with  $^{111}\text{In}$ . Lane 2 in Fig. 4A shows similar results for  $^{111}\text{In}$  binding to control DNA-DTPA after HPLC purification. The proportion of bound radioisotope in this case was 41%; thus, again, ca. 80% of the control DNA-DTPA was labeled with  $^{111}\text{In}$ . These data indicate that  $^{111}\text{In}$  binds effectively to PNA and DNA conjugates after HPLC purification. At the same time, since there were two DTPA molecules conjugated to each PNA molecule, only 40% of conjugated DTPA was occupied with  $^{111}\text{In}$  in the case of PNA. DNA molecules carried only one DTPA moiety; thus binding of radioisotope per conjugated DTPA moiety was almost twice as good for DNA-DTPA than for PNA-DTPA. The fact that DNA-DTPA binds more  $^{111}\text{In}$  per DTPA moiety than PNA-DTPA may be due to the large overall negative charge of the DNA molecule, which creates a higher local concentration of  $^{111}\text{In}^{3+}$  cations, facilitating their binding to DTPA.

#### PNA/DNA duplex formation

Figure 4B shows the duplex formation of target DNA with PNA-DTPA- $^{111}\text{In}$ , and control DNA-DTPA- $^{111}\text{In}$ , respectively. Lanes 1 and 3 are target DNA labeled by  $^{32}\text{P}$  at the 3' and the 5' end, respectively; lanes 2 and 4 are the mixtures of an excess PNA-DTPA- $^{111}\text{In}$  with target DNA labeled by  $^{32}\text{P}$  at the 3' and the 5' end, respectively; lane 5 is the mixture of control DNA-DTPA- $^{111}\text{In}$  with target DNA labeled by  $^{32}\text{P}$  at the 5' end. Binding of PNA molecule to the target DNA resulted in a larger shift in the gel mobility than did that of DNA to DNA (compare lanes 2 and 4 with lane 5). Importantly, the band-shift in the gel shows that in all cases more than 90% of the target was bound to  $^{111}\text{In}$ -DNA or -PNA.

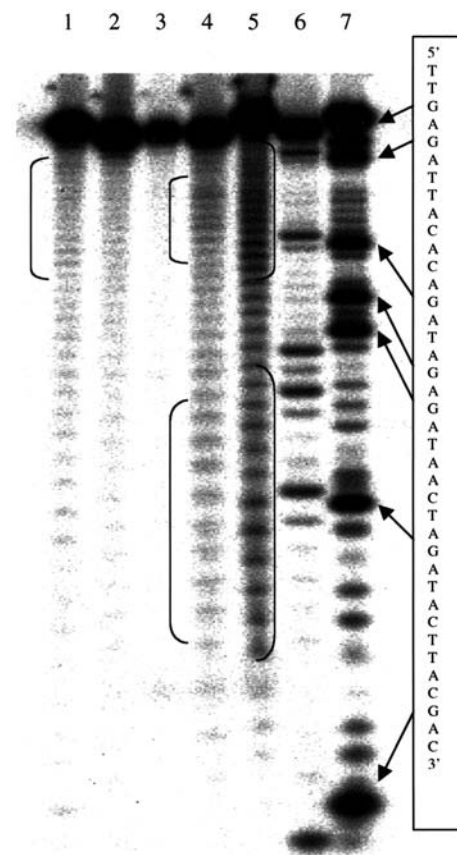


**Fig. 6.** Analysis of strand breaks in target via 12% denaturing PAGE. *Lanes:* 1, control DNA-DTPA- $^{111}\text{In}$ /target DNA 1- $^{32}\text{P}$ -5' duplex; 2, target DNA 1- $^{32}\text{P}$ -5'; 3, target DNA 1- $^{32}\text{P}$ -3'; 4, PNA 1-DTPA- $^{111}\text{In}$ /target DNA 1- $^{32}\text{P}$ -5' duplex; 5, PNA 1-DTPA- $^{111}\text{In}$ /target DNA 1- $^{32}\text{P}$ -3' duplex; 6, Maxam-Gilbert G sequencing line of target DNA 1- $^{32}\text{P}$ -5'; 7, Maxam-Gilbert G sequencing line of target DNA 1- $^{32}\text{P}$ -3'

To compare the stability of PNA/DNA and DNA/DNA duplexes, a competition experiment was performed with PNA 1 and control DNA binding to the target DNA 1. Figure 5 shows how the target DNA selected a complementary strand to form a more stable duplex in the presence of both complementary control DNA and PNA strands. Control DNA with target DNA did not form duplex in TE buffer (Tris/HCl-EDTA) at room temperature (lanes 4 and 5). However, lanes 6 and 7 indicated that PNA tends to displace control DNA from preformed duplex with target DNA to form a more stable PNA/DNA duplex in TE buffer at room temperature. This confirms that PNA binds more efficiently to target DNA than corresponding control DNA.

#### DNA strand breaks

Figure 6 shows the analysis of strand breaks in target DNA oligonucleotide labeled at the 5' end (lanes 1 and 4) or at the 3' end (lane 5) caused by either  $^{111}\text{In}$ -labeled

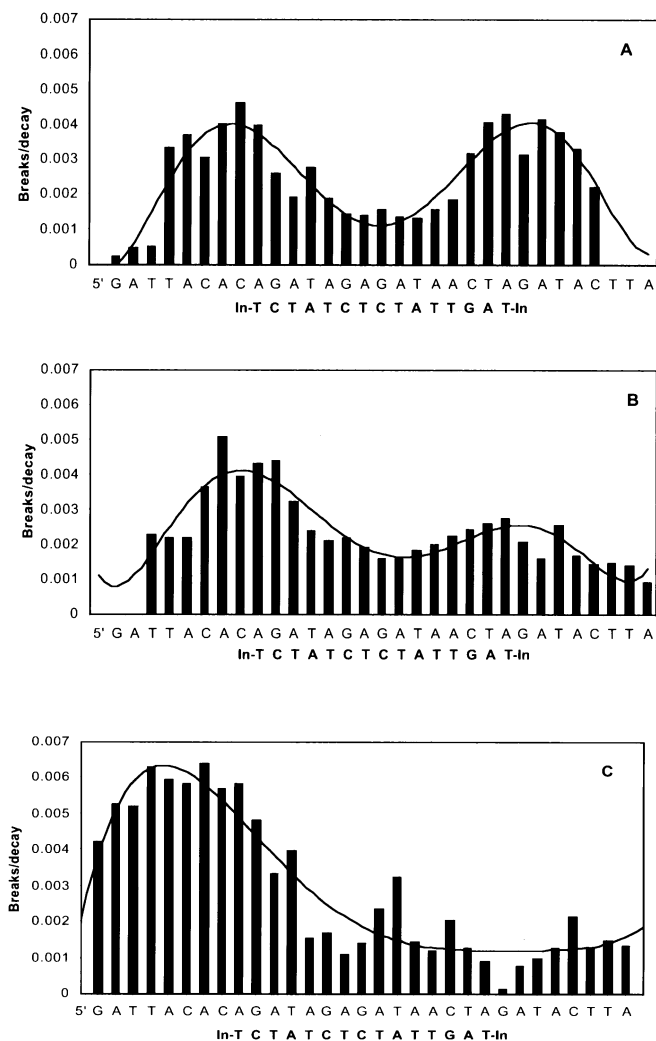


**Fig. 7A–C.** Distribution of PNA 1-DTPA-[ $^{111}\text{In}$ ]-induced strand breaks in target DNA 1- $^{32}\text{P}$ -5' (A, from lane 4 of Fig. 6) and target DNA 1- $^{32}\text{P}$ -3' (B, from lane 5 of Fig. 6), as well as the distribution of PNA 2-DTPA-[ $^{111}\text{In}$ ]-induced strand breaks in target DNA 2 (C)

control DNA (lane 1) or  $^{111}\text{In}$ -labeled PNA 1 (lanes 4 and 5). The positions of breaks were determined by comparison with the Maxam-Gilbert G-sequencing lanes (lanes 6 and 7) [10]. In the case of the radiolabeled PNA 1, breaks were distributed along the PNA-binding region of target DNA, with the regions of increased intensity at the ends (bracketed in Fig. 6). We determined the yield of breaks in this experiment as the percent of radioactivity of bands corresponding to breaks in relation to the total radioactivity, including the band of undamaged fragment [12]. When target DNA was labeled by  $^{32}\text{P}$  at the 5' end, the yield of breaks was 5.30%; when target DNA was labeled by  $^{32}\text{P}$  at the 3' end, the yield of breaks was 5.40%; the average total yield of breaks was 5.35%. The control DNA-DTPA-[ $^{111}\text{In}$ ] produced breaks in the target DNA with 1.9% yield (lane 1 in Fig. 6).

To estimate the frequencies of breaks per decay of  $^{111}\text{In}$  we performed the following calculations. The fraction of  $^{111}\text{In}$  that decayed in  $n$  days is  $1 - 2^{-n/t_{1/2}}$  where  $t_{1/2}=2.83$  days is the half-lifetime of  $^{111}\text{In}$  [12]. Thus, after 14 days,  $\sim 96\%$  of  $^{111}\text{In}$  decayed. Eighty percent of PNA-DTPA and DNA-DTPA were bound with  $^{111}\text{In}$ , and we assumed that 100% of the target DNA formed duplex. Thus, the frequency of strand breaks per decay was  $5.35\%/(80\% \times 96\%)=0.070$  for PNA 1/target DNA duplex, and  $1.9\%/(80\% \times 96\%)=0.025$  for control DNA/target DNA duplex. These results indicate that  $^{111}\text{In}$  caused a higher yield of DNA strand breaks per decay when delivered by PNA than when delivered by control DNA. This could be explained by the higher stability of PNA/DNA than DNA/DNA duplex structure, less overall negative charge of PNA/DNA duplex, and the lack of carbohydrate linker between DTPA and PNA, resulting in closer positioning of the  $^{111}\text{In}$  atom to the target DNA in the PNA/DNA duplex.

The frequencies of breaks at individual nucleotides were obtained by calculating the areas of Lorentz-type peaks fitted to the densitometrically generated intensity profiles of the lanes. The resulting strand break distributions for lanes 4 and 5 (Fig. 6) are shown in Fig. 7A, B. The distributions reveal two almost equal maxima of breaks opposite to the ends of PNA that are the sites of DTPA attachments and, therefore, the positions of  $^{111}\text{In}$ . These data demonstrate that the DTPA conjugated to both amines at the C terminus and N terminus, and that the bound  $^{111}\text{In}$  atoms were distributed almost equally between the termini.

In our previous studies [12], the DNA strand breaks per decay in a duplex model caused by DNA-DTPA-[ $^{111}\text{In}$ ] with a short C-3 linker attached in an internal position were as high as 0.38. There was a decrease in the yield of breaks when longer linkers (C-6 or C-7) attached in the terminal positions were used (0.05–0.06 strand breaks per decay in each DNA strand). Thus, the yield of breaks in the target DNA greatly depends on both the length and the position of the linker. Therefore, we expect that the use of a short internal linker for DTPA-[ $^{111}\text{In}$ ] conjugation to PNA will greatly improve the yield of breaks in future studies.

#### DNA strand breaks by PNA 2

In order to enhance the total yield of breaks per PNA oligomer, we used PNA 2 with three lysines at the C terminus (Table 1). After conjugation with cDTPAA, the corresponding PNA-DTPA complex was labeled with  $^{111}\text{In}$ , and the PNA-2/DNA duplex was made as described above. According to the ion-exchange HPLC and gel electrophoresis results, the conjugation yield of cDTPAA to PNA 2 was  $>80\%$ . Based on mass spectra analysis, we estimated that 23% of conjugates had one DTPA attached to PNA, 21% had two DTPAs attached to

PNA, 40% had three DTPAs attached to PNA and 16% had four DTPAs attached to PNA. Thus, on average 2.5 DTPAs per PNA 2 were conjugated. The gel-shift assays showed that about 90% of PNA-DTPA was labeled by  $^{111}\text{In}$ , and the target DNA was bound completely to form duplex (data not shown).

After 10 days (~91% of the  $^{111}\text{In}$  decayed) the target DNA strand breaks were determined by sequencing gel-electrophoresis as described for PNA 1 (data not shown) and a 6.8% yield of breaks was obtained. Thus, the yield of strand breaks per decay was  $6.83\%/(90\% \times 91\%) = 0.083$  for DNA duplex with  $^{111}\text{In}$ -labeled PNA 2. This indicates that  $^{111}\text{In}$  delivered by PNA 2 caused a higher yield of DNA strand breaks per decay than the corresponding PNA 1. Interestingly, only one maximum of strand breaks was observed (Fig. 7C). This suggests that either DTPA was attached mainly to the amino groups of the lysines of PNA 2 at the C terminus and/or  $^{111}\text{In}$  was preferably bound to the C-terminal DTPA. We conclude that addition of extra lysines to PNA increases the number of amino groups for DTPA conjugation, which increases the radioactivity that PNA can carry, resulting in the higher yield of DNA strand breaks. Our data also demonstrate that the  $^{111}\text{In}$ -loading efficiency and, therefore, yield of breaks, were higher for PNA 2 at the lysine-tagged PNA carboxy terminus.

### Concluding remarks

In summary, the cDTPAA moieties are readily conjugated to common mixed-base PNA oligomers at both termini through available PNA amino groups and PNA-DTPA conjugates can be effectively purified from the unreacted DTPA by HPLC. As a result, PNA can be loaded with  $^{111}\text{In}$  at high yield. The radionuclide, when delivered by PNA-DTPA conjugate to a specific site on single-stranded DNA, produces more breaks in target DNA per decay than when it is delivered by the corresponding DNA-DTPA conjugate.

Given the improved sequence specificity and binding affinity of PNA [21, 35], its chemical and biological stability [21, 27, 28, 29], and our latest data showing that site-specific breaks can be directed by radiolabeled ODNs to RNA strands as well [17], we expect that it will be possible to use PNA oligomers as radionuclide-carrying vehicles in antisense radiotherapeutic experiments. Recently, there has been significant progress in PNA cellular delivery that has substantially reduced the initial skepticism regarding the therapeutic and in vivo diagnostic use of PNAs [31, 36, 37, 38]. In addition, due to a neutral backbone, PNA appears to lack general toxicity and nonspecific protein binding [39, 40].

Although only one PNA sequence was involved in our proof-of-principle study, we do not expect any substantial limitations on the use of other PNAs for similar purposes, even given the well-known fact that not all

PNA sequences can readily be made. First, a range of possible sites normally exists for specific antisense/antigen application. Second, only the purine-rich PNAs (>60% purines) are usually difficult to synthesize or to handle, with G-rich oligomers typically being the worst. Yet, a study of very G-rich PNA recently reported by Datta et al. [41] found no problems while working with this PNA oligomer.

As to the possibility of using the radiolabeled PNAs in antigene approaches to treat malignant cells in a manner similar to treatment with radiolabeled triplex-forming ODNs [15, 17], the ability of mixed-base PNAs to invade duplex DNA under certain conditions is worth mentioning [42, 43, 44, 45]. Employment of mixed-base PNA in combination with PNA openers [46, 47] represents one more alternative for targeting oncogenes with radiolabeled PNAs. In this connection, recent advances in tissue/cell-specific PNA targeting [48, 49, 50] deserve attention. An alternative approach for DNA/RNA-targeted delivery of radioisotopes based on the use of other nonionic DNA analogues, morpholino oligomers [51, 52], is worthy of note in this context. These synthetic oligomers are also promising for future antisense/antigen radiotherapy trials although they exhibit some instabilities [51] and hybridize to nucleic acids less efficiently than PNAs [53].

*Acknowledgements.* We thank Peter E. Nielsen for kindly providing us with PNA oligomer used in the pilot experiments and William Eckelman and Chang Paik for critical reading of the manuscript. This work was partially supported by Boston Univ. SPRInG award to V.V.D. Igor G. Panyutin and Vadim V. Demidov should be jointly regarded as corresponding authors.

### References

- Weiner RE, Thakur ML. Radiolabeled peptides in the diagnosis and therapy of oncological diseases. *Appl Radiat Isot* 2002; 57:749–763.
- Swift P. Novel techniques in the delivery of radiation in pediatric oncology. *Pediatr Clin North Am* 2002; 49:1107–1129.
- Juwaid ME. Radioimmunotherapy of B-cell non-Hodgkin's lymphoma: from clinical trials to clinical practice. *J Nucl Med* 2002; 43:1507–1529.
- Hnatowich DJ. Antisense and nuclear medicine. *J Nucl Med* 1999; 40:693–703.
- Pardridge WM. Antisense radiopharmaceuticals: agents for imaging gene expression. *Drug Discov Today* 2001; 6:104–106.
- Panyutin IG, Neumann RD. Sequence-specific DNA double-strand breaks induced by triplex forming  $^{125}\text{I}$  labeled oligonucleotides. *Nucleic Acids Res* 1994; 22:4979–4982.
- Panyutin IG, Neumann RD. Sequence-specific DNA breaks produced by triplex-directed decay of iodine-125. *Acta Oncol* 1996; 35:817–823.
- Karamychev VN, Panyutin IG, Reed MW, Neumann RD. Effect of radionuclide linker structure on DNA cleavage by  $^{125}\text{I}$ -labeled oligonucleotides. *Antisense Nucleic Acid Drug Dev* 1997; 7:549–557.

9. Panyutin IG, Neumann RD. Gene radiotherapy; gene targeted versus targeted by gene product. *J Nucl Med* 1998; 39:928–929.
10. Sedelnikova OA, Panyutin IG, Thierry AR, Neumann RD. Radiotoxicity of iodine-125-labeled oligodeoxyribonucleotides in mammalian cells. *J Nucl Med* 1998; 39:1412–1418.
11. Karamychev VN, Reed MW, Neumann RD, Panyutin IG. Distribution of DNA strand breaks produced by iodine-123 and indium-111 in synthetic oligodeoxynucleotides. *Acta Oncol* 2000; 39:687–692.
12. Karamychev VN, Panyutin IG, Kim MK, et al. DNA cleavage by <sup>111</sup>In-labeled oligodeoxyribonucleotides. *J Nucl Med* 2000; 41:1093–1101.
13. Sedelnikova OA, Panyutin IG, Luu AN, et al. Targeting the human *mdr1* gene by <sup>125</sup>I-labeled triplex-forming oligonucleotide. *Antisense Nucleic Acid Drug Dev* 2000; 10:443–452.
14. Panyutin IG, Winters TA, Feinendegen LE, Neumann RD, et al. Development of DNA-based radiopharmaceuticals carrying Auger-electron emitters for anti-gene radiotherapy. *Q J Nucl Med* 2000; 44:256–267.
15. Panyutin IV, Luu AN, Panyutin IG, Neumann RD. Strand breaks in whole plasmid DNA produced by the decay of <sup>125</sup>I in a triplex-forming oligonucleotide. *Radiat Res* 2001; 156:158–166.
16. Sedelnikova OA, Luu AN, Karamychev VN, Panyutin IG, Neumann RD. Development of DNA-based radiopharmaceuticals carrying Auger-electron emitters for antigenic radiotherapy. *Int J Radiat Oncol Biol Phys* 2001; 49:391–396.
17. Gaidamakova EK, Neumann RD, Panyutin IG. Site-specific strand breaks in RNA produced by <sup>125</sup>I radiodecay. *Nucleic Acids Res* 2002; 30:4960–4965.
18. Sedelnikova OA, Karamychev VN, Panyutin IG, Neumann RD. Sequence-specific gene cleavage in intact mammalian cells by <sup>125</sup>I-labeled triplex-forming oligonucleotides conjugated with nuclear localization signal peptide. *Antisense Nucleic Acid Drug Dev* 2002; 12:43–49.
19. Nielsen PE, Egholm M, Berg RH, Buchardt O. Sequence selective recognition of DNA by strand displacement with a thymine-substituted polyamide. *Science* 1991; 254:1497–1500.
20. Egholm M, Buchardt O, Christensen L, et al. PNA hybridizes to complementary oligonucleotides obeying the Watson-Crick hydrogen-bonding rules. *Nature* 1993; 365:566–568.
21. Uhlmann E, Peyman A, Breipohl G, Will DW. PNA: synthetic polyamide nucleic acids with unusual binding properties. *Angew Chem Int Ed Engl* 1998; 37:2796–2823.
22. Ray A, Nordén B. Peptide nucleic acid (PNA): its medical and biotechnological applications and promise for the future. *FASEB J* 2000; 14:1041–1060.
23. Demidov VV, Frank-Kamenetskii MD. Sequence-specific targeting of duplex DNA by peptide nucleic acids via triplex strand invasion. *Methods* 2001; 23:108–122.
24. Demidov VV, Yavnilovich MV, Belotserkovskii BP, Frank-Kamenetskii MD, Nielsen PE. Kinetics and mechanism of polyamide (peptide) nucleic acid binding to duplex DNA. *Proc Natl Acad Sci U S A* 1995; 92:2637–2641.
25. Demidov VV, Yavnilovich MV, Frank-Kamenetskii MD. Kinetic analysis of specificity of duplex DNA targeting by homopyrimidine PNAs. *Biophys J* 1997; 72:2763–2769.
26. Hanvey JC, Peffer NJ, Bisi JE, et al. Antisense and antigene properties of peptide nucleic acids. *Science* 1992; 258:1481–1485.
27. Demidov VV, Potaman VN, Frank-Kamenetskii MD, Egholm M, Buchardt O, Sönnichsen SH, Nielsen PE. Stability of peptide nucleic acids in human serum and cellular extracts. *Biochem Pharmacol* 1994; 48:1310–1313.
28. Efimov VA, Choob MV, Buryakova AA, Kalinkina AL, Chakhmakheva OG. Synthesis and evaluation of some properties of chimeric oligomers containing PNA and phosphono-PNA residues. *Nucleic Acids Res* 1998; 26:566–575.
29. Kristensen E. In vitro and in vivo studies on pharmacokinetics and metabolism of PNA constructs in rodents. In: Nielsen PE, ed. *Peptide nucleic acids: methods and protocols*. Totowa, NJ: Humana Press; 2002:259–269.
30. Appendix: quantification. In: Nielsen PE, Egholm M, eds. *Peptide nucleic acids: protocols and applications*. Wymondham, Norfolk, UK: Horizon Scientific Press; 1999:2550.
31. Braasch DA, Corey DR. Synthesis, analysis, purification, and intracellular delivery of peptide nucleic acids. *Methods* 2001; 23:97–107.
32. Lewis MR, Jia F, Gallazzi F, et al. Radiometal-labeled peptide-PNA conjugates for targeting *bcl-2* expression: preparation, characterization, and in vitro mRNA binding. *Bioconjugate Chem* 2002; 13:1176–1180.
33. Ørum H, Casale R, Egholm M. Labeling of PNA. In: Nielsen PE, Egholm M, eds. *Peptide nucleic acids: protocols and applications*. Wymondham, Norfolk, UK: Horizon Scientific Press; 1999:81–86.
34. Garcia BA, Heaney PJ, Tang K. Improvement of the MALDI-TOF analysis of DNA with thin-layer matrix preparation. *Anal Chem* 2002; 74:2083–2091.
35. Armitage BA. The impact of nucleic acid secondary structure on PNA hybridization. *Drug Discov Today* 2003; 8:222–228.
36. Braasch DA, Corey DR. Lipid-mediated introduction of peptide nucleic acids into cells. *Methods Mol Biol* 2002; 208:211–223.
37. Koppelhus U, Nielsen PE. Cellular delivery of peptide nucleic acid (PNA). *Adv Drug Deliv Rev* 2003; 55:267–280.
38. Mier W, Eritja R, Mohammed A, Haberkorn U, Eisenhut M. Peptide-PNA conjugates: targeted transport of antisense therapeutics into tumors. *Angew Chem Int Ed Engl*. 2003; 42:1968–1971.
39. Pardridge WM, Boado RJ, Kang Y-S. Vector-mediated delivery of a polyamide (“peptide”) nucleic acid analogue through the blood-brain barrier in vivo. *Proc Natl Acad Sci USA* 1995; 92:5592–5596.
40. Hamilton SE, Iyer M, Norton JC, Corey DR. Specific and non-specific inhibition of transcription by DNA, PNA and phosphorothioate promoter analog duplexes. *Bioorg Med Chem Lett* 1996; 6:2897–2900.
41. Datta B, Schmitt C, Armitage BA. Formation of a PNA<sub>2</sub>-DNA<sub>2</sub> hybrid quadruplex. *J Am Chem Soc* 2003; 125:4111–4118.
42. Boffa LC, Carpaneto EM, Allfrey VG. Isolation of active genes containing CAG repeats by DNA strand invasion by a peptide nucleic acid. *Proc Natl Acad Sci USA* 1995; 92:1901–1905.
43. Zhang X, Ishihara T, Corey DR. Strand invasion by mixed base PNAs and a PNA-peptide chimera. *Nucleic Acids Res* 2000; 28:3332–3338.
44. Kaihatsu K, Braasch DA, Cansizoglu A, Corey DR. Enhanced strand invasion by peptide nucleic acid-peptide conjugates. *Biochemistry* 2002; 41:11118–11125.
45. Demidov VV, Protozanova E, Izvolsky KI, Price C, Nielsen PE, Frank-Kamenetskii MD. Kinetics and mechanism of the DNA double helix invasion by pseudocomplementary peptide nucleic acids. *Proc Natl Acad Sci USA* 2002; 99:5953–5958.
46. Demidov VV. PNA openers for duplex DNA: basic facts, fine tuning and emerging applications. In: Nielsen PE, ed.

- Peptide nucleic acids: protocols and applications, 2nd edn. Wymondham, Norfolk, UK: Horizon Bioscience; 2004:207–226.
47. Broude NE, Demidov VV, Kuhn H, Gorenstein J, Pulyaeva H, Volkovitsky P, Drukier AK, Frank-Kamenetskii MD. PNA openers as a tool for direct quantification of specific targets in duplex DNA. *J Biomol Struct Dynam* 1999; 17:237–244
  48. Boffa LC, Scarfi S, Mariani MR, et al. Dihydrotestosterone as a selective cellular/nuclear localization vector for anti-gene peptide nucleic acid in prostatic carcinoma cells. *Cancer Res* 2000; 60:2258–2262.
  49. Zhang X, Simmons CG, Corey DR. Liver cell specific targeting of peptide nucleic acid oligomers. *Bioorg Med Chem Lett* 2001; 11:1269–1272.
  50. Lee HJ, Boado RJ, Braasch DA, Corey DR, Pardridge WM. Imaging gene expression in the brain in vivo in a transgenic mouse model of Huntington's disease with an antisense radiopharmaceutical and drug-targeting technology. *J Nucl Med* 2002; 43:948–956.
  51. Liu C, Liu G, Liu N, Zhang YM, He J, Rusckowski M, Hnatowich DJ. Radiolabeling morpholinos with  $^{90}\text{Y}$ ,  $^{111}\text{In}$ ,  $^{188}\text{Re}$  and  $^{99\text{m}}\text{Tc}$ . *Nucl Med Biol* 2003; 30:207–214.
  52. Liu G, Liu C, Zhang S, He J, Liu N, Gupta S, Rusckowski M, Hnatowich DJ. Investigations of  $^{99\text{m}}\text{Tc}$  morpholino pretargeting in mice. *Nucl Med Commun* 2003; 24:697–705.
  53. Braasch DA, Corey DR. Novel antisense and peptide nucleic acid strategies for controlling gene expression. *Biochemistry* 2002; 41:4503–4510.